Ab Initio Analysis of the Structural Properties of Alkyl-Substituted Polyhedral Oligomeric Silsesquioxanes

Hung-Chih Li,[†] Cheng-Ying Lee,[‡] Clare McCabe,*[,†] Alberto Striolo,[†,§] and Matthew Neurock[‡]

Department of Chemical Engineering, Vanderbilt University, Nashville, Tennessee 37235, and Department of Chemical Engineering, University of Virginia, Charlottesville, Virginia 22904-4741

Received: November 4, 2006; In Final Form: February 25, 2007

Ab initio quantum mechanical calculations have been performed to establish the potentials for alkyl-substituted polyhedral oligomeric silsesquioxane (POSS) monomers $R_xH_{8-x}(SiO_{1.5})_8$. More specifically, we have examined the unsubstituted POSS $(SiO_{1.5}H)_8$ cage as well as linear and cyclic alkyl-substituted cages where one of the terminating hydrogen atoms is replaced by a hydrocarbon group, that is, $R_1H_7(SiO_{1.5})_8$. The results for the minimum-energy configurations indicate that the presence of the linear hydrocarbon chains and cyclic intermediates have very little effect on the structure of the POSS cage. Although the POSS monomeric cage does influence the partial charges of the first few carbon atoms covalently bound to the POSS monomer, its effect on the structural properties of the alkyl chain is small. Differences arise, however, for cyclic alkyl substitutents bound to the POSS cage due to the repulsive interactions between the POSS cage and bulkier cyclic intermediates that result upon rotation of the Si−C−C−C dihedral angles. The interatomic potentials for these rotational, or torsional, terms need to be modified slightly in order to appropriately simulate sterically hindered substitutents on the cage. Our results suggest that combining an atomistic force field independently developed to describe silsesquioxanes with an independent atomistic model developed to describe hydrocarbon chains can be used in classical molecular simulation studies of most alkyl-silsesquioxanes. This avoids the need to develop specific force fields for each substituted POSS cage studied and opens up the possibility of using molecular simulation to probe the thermodynamic and structural properties of these unique nanoscale building blocks.

Introduction

Interest in polyhedral oligomeric silsesquioxane molecules (POSS)[1] has grown considerably in recent years because they offer the opportunity to construct monodisperse organic−inorganic nanobuilding blocks, which opens up a variety of possible applications such as the reinforcement of polymeric materials,[2−6] production of self-assembled nanoparticles,[7−9] preparation of thin films,[10,11] and generation of lamellar structures.[12,13] POSS monomers consist of silicon and oxygen atoms arranged into a cubic or cage-like structure such that the silicon atoms are located at the corners of the cage with the oxygen atoms along the bonds. In Figure 1a, we report a schematic representation of the smallest "bare" POSS monomer in which the silicon atoms are terminated with hydrogens giving a chemical formula of $(SiO_{1.5})_8H_8$. The wide variety of applications for POSS-based materials arises from the ease by which the hydrogen atoms can be substituted with functional groups such as alcohols, phenols, alkoxysilanes, chlorosilanes, epoxides, esters, isocyanates, and so forth.[14] Through the manipulation of the functional groups on the POSS cage, as well as the size and shape of the POSS cage itself, it is possible to modulate the physical properties of POSS monomers, such as their dissolution in various solvents and/or polymeric materials.[15]

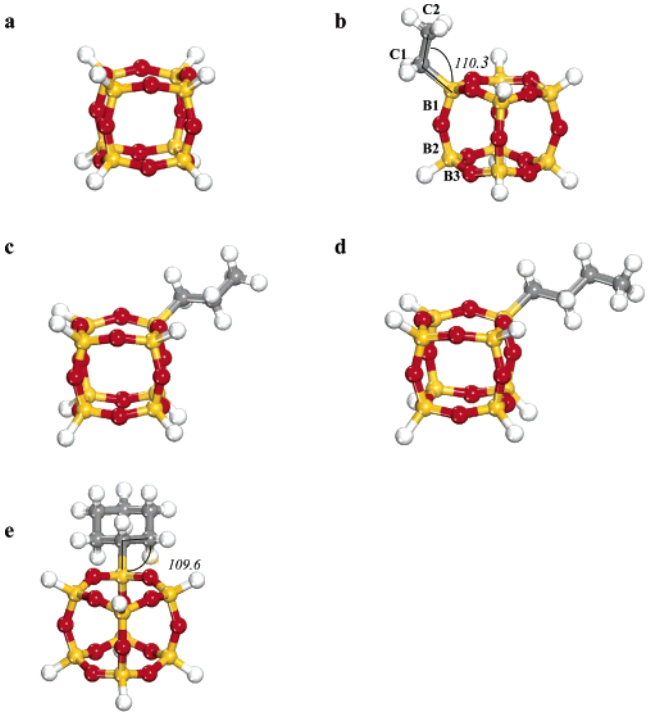

Figure 1. Structural illustration of POSS molecules: (a) bare POSS, (b) ethyl-POSS, (c) propyl-POSS, (d) butyl-POSS, (e) cyclohexyl-POSS. Orange, red, white, and gray spheres represent silicon, oxygen, hydrogen, and carbon atoms, respectively.

Molecular simulation appears to be an ideal tool for improving our understanding of POSS-based hybrid materials due to the

* Author to whom all correspondence should be addressed. E-mail: c.mccabe@vanderbilt.edu. Tel: 615 322-6853. Fax: 615 343-7951.
[†] Vanderbilt University.
[‡] University of Virginia.
[§] Present address: School of Chemical Biological and Materials Engineering, University of Oklahoma, Norman, OK 73019.

10.1021/jp0672757 CCC: $37.00
Published on Web 04/19/2007

complexity of performing experiments at the nanoscale. Additionally, simulation allows us to probe the molecular-level behavior that is critical to understanding nanoscale interactions for these hybrid materials. Although extensive experimental work has demonstrated, or at least suggested, many possible applications for POSS-based materials, theoretical studies on these compounds have emerged much more slowly. Notably, Choi and co-workers in a combined experimental and mesoscale simulation study of epoxy resins showed that flexible tethers on the POSS cage are responsible for lower glass transition temperatures and elastic moduli but provide higher fracture toughness, whereas rigid tethers provide larger glass transition temperatures and elastic moduli but poor fracture toughness.[16] In related work, Bharadwaj et al. used molecular dynamics simulations to study norborene-POSS polymers.[17] Their results suggested that the thermal and elastic properties of POSS-containing polymers are enhanced because POSS monomers inhibit the motion of polymer chains. In previous work, we have studied the crystal structure, melting temperature,[18,19] and thermodynamic and transport properties of POSS monomers dissolved in hexane, hexadecane, and poly(dimethyl siloxane) using classical molecular dynamics simulation.[20−23] In this, and the other simulation studies discussed, inter- and intramolecular potentials were obtained by combining potentials that were developed independently for the different chemical components of a POSS monomer, even though no theoretical study assures that this procedure yields reliable results. Such theoretical "reassurance" can only be obtained through higher-level electronic-structure calculations for different silsesquioxanes, which is the focus of the current work.

Previous electronic-structure calculations have investigated the mechanism for the synthesis of silsesquioxanes[24] and were used to derive a consistent force field for typical structural elements of zeolites including silica cages.[25] Xiang et al.[26] showed that the nonlocal density approximation is required to reliably predict the most stable silsesquioxane isomers. They also investigated the highest occupied and lowest unoccupied molecular orbitals (HOMO and LUMO, respectively) and showed that for all the silsesquioxanes considered the HOMOs were composed of oxygen p-type atomic orbitals, while LUMOs depend on the molecular size. The theoretical stability of silica cages of different sizes has also been investigated by ab initio methods. In agreement with experimental evidence, Earley[27] found that molecules containing $(Si-O)_3$ rings are significantly less stable than molecules containing only larger rings. Wichmann and Jug[28] studied silsesquioxane cages containing an increasing number of silicon atoms to investigate the growth mechanism for these molecules and were able to reproduce the geometric parameters of $(SiO_{1.5})_8H_8$ cages in reasonable agreement with experimental data. The electronic properties of $(SiO_{1.5})_8H_8$ POSS monomers chemisorbed on silica surfaces have also been studied by Car−Parrinello ab initio simulations.[29] Experimental studies for the adsorption of atomic hydrogen in POSS materials[30] triggered theoretical studies on the trapping and detrapping mechanisms of atoms or molecules in POSS monomers. Mattori et al.[31] illustrated the mechanism by which hydrogen atoms can penetrate and reside within a POSS monomer without causing a significant deformation to its molecular structure. Tejerina and Gordon[32] found that the energy barrier for insertion of molecular nitrogen and oxygen into $(SiO_{1.5})_8H_8$ monomers is close to the dissociation enthalpy of the Si−O bond but that insertion may be feasible in larger POSS monomers. Experimental evidence demonstrates that metal-substituted POSS molecules possess catalytic activity;[33,34] thus, recent theoretical interest has been focused on titanium-substituted POSS molecules that have similar structures compared to the silicon homologues but appear to be more stable.[35] Current interest is shifting toward understanding the electronic and structural properties of substituted POSS systems in which any number of hydrogen atoms are substituted with different functional groups. For example, alkyl silsesquioxanes are found to be stable, even though their stability decreases as the size of the molecules increases above $(SiO_{1.5})_8(CH_3)_8$.[36]

To build a molecular-level understanding of POSS systems and their interactions, we examine two basic questions in this work: do the geometric structural features of the POSS monomer depend on the substituents attached at its corners, and how do the properties of the tethered substituents change when they are covalently bound to a POSS monomer? In this work, we have focused on monosubstituted POSS molecules, primarily because of their simplicity, though such systems have been studied experimentally and show potentially interesting properties, such as their use as amphiphiles for novel core/shell type silicate nanoparticles.[37] In particular, in this work we have performed ab initio electronic-structure calculations on the smallest unsubstituted cubic POSS monomer (Figure 1a) and for POSS monomers where one hydrogen atom has been substituted by short linear alkyl chains (Figure 1b−d) as well as more sterically constrained cylcohexyl tethers (Figure 1e). In what follows, we optimize the monosubstituted cubic POSS systems and establish the relevant structural potentials including bond stretching (Si−C), angle bending (Si−C−C and O−Si−C), and torsional angle rotations (O−Si−C−C, and Si−C−C−C). In addition, we determine a set of partial charges to assign to each atom in the molecules considered. We discuss to what extent the geometric and electronic properties of POSS cages are affected by the substituents and to what extent the properties of a hydrocarbon chain are altered when it is covalently bound to a POSS cage.

Computational Methods

Electronic-structure calculations have been performed to obtain structures for the bare POSS $(SiO_{1.5}H)_8$ cage and different monosubstituted alkyl POSS molecules, along with information on the equilibrium bond lengths, bond angles, and dihedral angles, and the partial charge distributions for these systems.

HF and MP2 wave function calculations were carried out on the basic POSS cage (Figure 1a) and the ethyl- (Figure 1b), propyl- (Figure 1c), and butyl- (Figure 1d) substituted POSS using Gaussian 98.[38] The structures were optimized using restricted HF. Subsequently, single-point MP2 calculations were carried out on each of the optimized structures to determine the corresponding energies. All calculations were performed using the cc-pVDZ basis set.

Calculations were also performed using gradient-corrected density functional theory on all of the POSS monomers studied (Figure 1a−e). All of the DFT calculations reported herein were performed using DMol[39] with all electron double-numerical-polarized (DNP) basis sets with relativistic correction and the revised Perdew−Burke−Ernzerhof (RPBE)[40] generalized gradient approximation for the exchange-correlation potential. The wave functions were confined within a 4.0 Å real space cutoff. The electronic density was converged within each self-consistent field iteration to within 1×10^{-5} au, and the geometry was converged to within 2×10^{-5} au.

Additionally, atomic partial charges have been estimated from the results of the MP2 calculations. A common estimation method is Mulliken analysis;[41] however, the results can be

TABLE 1: Selected Geometric Parameters Computed for Bare POSS Monomers $(SiO_{1.5})_8H_8$[a]

reference		Si-O bond/Å	Si-H bond/Å	Si−O−Si angle	O-Si-O angle
this work	DFT	1.654	1.467	146.8°	110.1°
	Gaussian 98 (HF)	1.650	1.462	148.7°	109.1°
Hill and Sauer[24] (DFT)		1.626		150°	
Earley[27] (QM)		1.630		149°	109.1°
Wichmann and Jug[28] (semiempirical)		1.609	1.467	146.7°	108.6°
Mattori et al.[31] (DFT)		1.64	1.46	148.2°	109.6°
Xiang et al.[26] (DFT)		1.68		144.6°	111.3°
Tejerina and Gordon[32] (QM)		1.624	1.455	150.5°	108.4°
Lin et al.[56] (DFT)		1.598	1.449	149.1°	109.1°
Pasquarello et al.[29] (DFT/LDA)		1.62	1.51	148.6°	109.4°
		experimental			
Auf der Heyde et al.[51]*		1.62		147.5−147.6°	109.4−109.7°
Earley[52]*		1.619		148°	
Törnroos[53]*		1.623−1.628	1.459−1.463	147.25−147.45°	109.07−109.86°

[a] Results obtained in this work are here compared to results from the literature for both ab initio studies (the nature of which are given in brackets) and experimental investigations. Experimental references are indicated by the symbol "*" in the table.

TABLE 2: Geometric Parameters Computed for Bare and Monosubstituted Alkane Silsesquioxanes from DFT and (Gaussian 98 HF) Results

	Si−O (B1)/Å	Si−O (B2)/Å	Si−O (B3)/Å	Si−O−Si	O−Si−O	Si−C/H	C1−C2	O−Si−C	Si−C−C	O−Si−C−C	Si−C−C−C
POSS	1.654 (1.650)	1.654 (1.650)	1.654 (1.650)	146.8 (148.7)	110.1 (109.1)	1.467					
ethyl-POSS	1.661 (1.655)	1.650 (1.647)	1.655 (1.650)	148.2(149.2)	109.0 (108.3)	1.865	1.548	110.3	115.5	−175.8	
propyl-POSS	1.661(1.656)	1.649 (1.646)	1.655 (1.650)	148.2(149.8)	109.0 (108.2)	1.865	1.549	110.0	115.9	178.3	176.9
butyl-POSS	1.661	1.649	1.655	148.2	109.0	1.864	1.548	109.9	116.5	−179.4	−179.0
cyclohexyl-POSS	1.663	1.649	1.655	148.3	108.8	1.872	1.557	110.0	112.5	177.4	−179.0

[a] B1 is for the Si−O bonds with the Si atom being the one to which the alkane group is attached; B2 is for the next closest Si−O bonds having an O atom in common with B1; B3 is for the next closest Si−O bonds sharing a Si atom with B2. C1 is the C atom attached to the Si atom, and C2 is the C atom next to C1. This nomenclature is shown on the monosubstituted POSS monomer shown in Figure 1b.

dependent on the basis set employed and there is no unambiguous way to assign charge to two atoms within a bond.[42] An alternative approach is to fit the point charges at preselected positions to the electrostatic potential surface;[43−46] however, the partial charges obtained can depend on the molecular conformation considered.[47,48] Approaches used to circumvent this problem involve restricting the partial charges to a targeted set of charges or to a set of charges that can reproduce a desired property such as the molecular dipole moment,[49] or by including multipole analysis to enrich the modified population analysis used in the Mulliken method.[41] Another possibility, which has been used in this work, involves evaluating the partial charges for several different molecular conformations and then averaging the results according to Boltzmann statistics.[48] For each molecular conformation, the atomic charge was obtained with the Merz−Singh−Kollman algorithm.[42,50] Weighted averages for the partial charges, located at the centers of mass of each atom were then calculated using the expression

$$\overline{q} = \frac{\sum_i q_i \exp\left(-\frac{E_i}{kT}\right)}{\sum_i \exp\left(-\frac{E_i}{kT}\right)} \quad (1)$$

evaluated at $T = 300$ K, where the summation is over all of the conformations tested.

Results and Discussion

Structural Properties. In Table 1, we report the structural parameters obtained from our calculations at different levels of theory for the bare POSS monomer ($(SiO_{1.5})_8H_8$), which includes the Si−O and Si−H bond lengths and the Si−O−Si and O−Si−O angles that were calculated herein to be 1.654 (1.650) Å, 1.467 (1.462) Å, 146.8 (148.7)°, and 110.1 (109.1)°, respectively, at the DFT (and Gaussian 98 HF) levels. The results of our calculations are in very good agreement with theoretical results reported previously from other methods and experimental X-ray diffraction data.[51−53] Nevertheless, it should be remembered that the electronic structure calculations were performed on a single molecule in vacuum while the experimental data were obtained from single-crystal studies.

To understand the effect that an alkyl substituent exerts on the structural features of POSS cages, we substituted one of the hydrogen atoms on the bare POSS monomer (Figure 1a) with hydrocarbon chains of different lengths. We considered the ethyl-, propyl-, and butyl-POSS systems (Figure 1b−d, respectively). In addition, we examined the influence of steric considerations by using a cyclic aliphatic substituent, that is, a cyclohexyl group (Figure 1e). We report in Table 2 the optimized structural parameters for the bare (Figure 1a) and monosubstituted alkyl-POSS cages (Figure 1b−e) determined from the DFT and Gaussian 98 HF calculations. These include the Si−C bond length, the Si−O bond lengths, the O−Si−O angles (where the silicon atom is covalently bound to the hydrocarbon chain), the Si−O−Si angle (where one of the silicon atoms is covalently bound to the hydrocarbon chain), the C−C bond lengths, the O−Si−C bond angle, the Si−C−C bond angle, the C−C−C bond angles, the Si−C−C−C dihedral angle, and the O−Si−C−C dihedral angle. The results indicate that structural changes that occur in the POSS cage itself upon the substitution of a single terminal hydrogen atom with an alkyl substituent are localized and very small. Furthermore, there is essentially no influence of chain length on these results because the ethyl, propyl, butyl, and cyclohexyl groups all lead to very similar structures for the POSS cage.

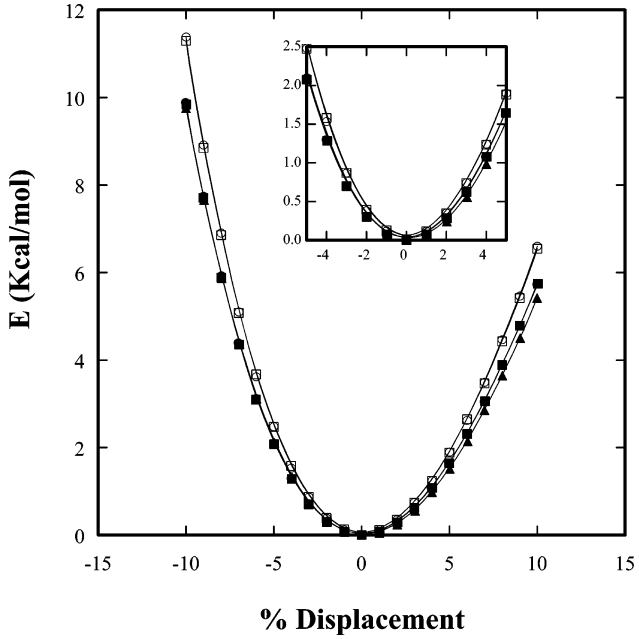

Figure 2. Si−C stretching potentials for ethyl-, propyl-, and cyclohexyl-POSS monomers. Filled circles, squares, and triangles are results from DFT for ethyl-, propyl-, and cyclohexyl-POSS, respectively. Included for comparison are the results from Gaussian 98 MP2 calculations for ethyl-POSS (open circles) and propyl-POSS (open squares). The solid line is a harmonic fitting to the results in proximity of the equilibrium bond length. The inset shows a magnified view of the results around the minimum.

Potential Energy Curves. Although there is little change in the POSS cube upon substitution, there may be changes in the structure of the alkyl substituents due to the presence of the POSS cage. Herein, we compare changes in the bond stretching, angle bending, and torsional angle potentials for the structural features closest to the Si−C contact for the linear alkyl-POSS (Figure 1b−d) and the constrained cyclohexyl-POSS (Figure 1e) systems. Given the similarity between the structural results from the DFT and Gaussian 98 calculations, only the results from the DFT calculations are discussed in the text; the Gaussian 98 MP2 results are included where practical in the figures for comparison. We also provide comparisons with well-known hydrocarbon potentials to examine the differences that would result due to the influence of the POSS cage.

i. Si−C Stretching Potential. We focus first on the properties of the Si−C bond. The optimized Si−C bond length was calculated from DFT to be 1.854 Å for the ethyl substituent (Figure 1b) and 1.870 Å for the cyclohexyl substituent (Figure 1e). Despite the changes in the magnitude of the Si−C bond length between the POSS cage and the alkyl substituent, the form of the potential remains similar. Figure 2, for example, shows the energy cost corresponding to the stretching of the Si−C bond from its equilibrium position for the ethyl-, propyl-, and cyclohexyl-POSS monomers. The results in all three cases indicate that a displacement from the equilibrium position of ±5% of the bond length increases the bond energy by approximately 2 kcal/mol. As might be expected, the results indicate that it is easier to elongate the Si−C bond between the alkyl substituent and the POSS cage rather than compress it. The results in Figure 2 for ethyl-, propyl-, and cyclohexyl-POSS are essentially indistinguishable, supporting the observation that the length of the hydrocarbon tether does not influence the geometric properties of the POSS monomer. In addition, the results for the cyclohexyl-POSS suggest that steric features of the tether do not change the resulting Si−C stretching potential.

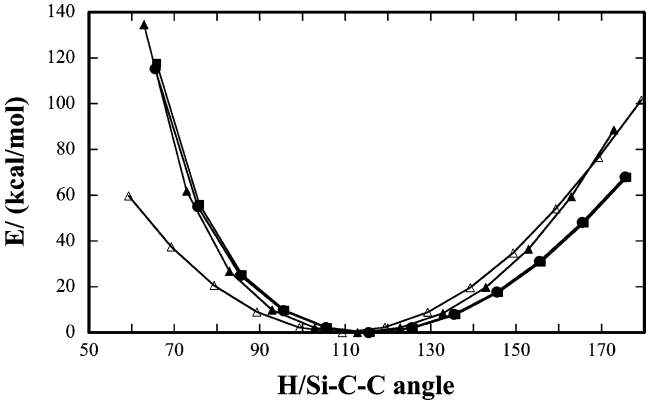

Figure 3. Si−C−C bending potentials from DFT for ethyl-POSS (filled circles), propyl-POSS (filled squares), and cyclohexyl-POSS (filled triangles) monomers. Results for the H−C−C bending potential in cyclohexane are represented by open triangles.

Toward the development of an atomistic force field for POSS, we also noted that the increase in bond energy when the Si−C bond length varies between ±5% from the equilibrium position can be described by a harmonic analytical model. The results presented in Figure 2 show that the Si−C bond potentials can be described by stiff analytical functions; thus, it is unlikely for these quantities to assume values far from the equilibrium parameters.

ii. Si−C−C Angle Bending Potential. Si−C−C angle bending potentials for ethyl-POSS (Figure 1b), cyclohexyl-POSS (Figure 1e), and cyclohexane are reported in Figure 3. The optimal Si−C−C (H−C−C) bond angles are 115.5° for ethyl-POSS, 115.9° for propyl-POSS, 112.9° for cyclohexyl-POSS, and 109.3° for cyclohexane. The shift between cyclohexyl-POSS and cyclohexane is 3°. All four cases take on a parabolic-shaped potential energy surface well centered at the equilibrium position. The shapes and energy penalties for ethyl- and cyclohexyl-POSS are alike in that decreasing the angle from its optimal point (negative angle deviations) suffers a greater energy penalty than increasing it from its optimal value (positive angle deviations) because of the more repulsive interactions that take place between the tether and the cage for the former case. For example, cyclohexyl-POSS has a potential energy of 34 kcal/mol at +50° but 68 kcal/mol at −50°. The potential curve for cyclohexyl-POSS is steeper than ethyl-POSS because of the stronger repulsive interactions between the bulkier cyclohexyl tether and the cage. The potential for rotation about a C−H bond of cyclohexane, however, is quite shallow in comparison with that for the substituted-POSS system. This is due to the loss of the steric repulsive interactions when we substitute the POSS cage here with a hydrogen atom. The cyclohexane potential is not only shallower but also much more symmetric about its optimal value, which is due to the symmetry of the molecule about its C−H bond. Note that the ethyl- and propyl-POSS potentials are indistinguishable within ±20° of deviation from their equilibrium positions with an energy penalty of 10 kcal/mol.

iii. O−Si−C Angle Bending Potential. We report calculated O−Si−C bending potentials for ethyl- (Figure 1b), propyl- (Figure 1c), and cyclohexyl-POSS (Figure 1e) monomers in Figure 4. The equilibrium O−Si−C angles are 110.3° for ethyl-POSS, 110.0° for propyl-POSS, and 109.6° for cyclohexyl-POSS. All three monomers have similarly shaped potentials in which negative angle deviations suffer a greater energy penalty than positive angle deviations because of stronger repulsive interactions between the tether and the cage for the former case. Cyclohexyl-POSS has a slightly steeper potential well than ethyl- and propyl-POSS because of the stronger repulsive

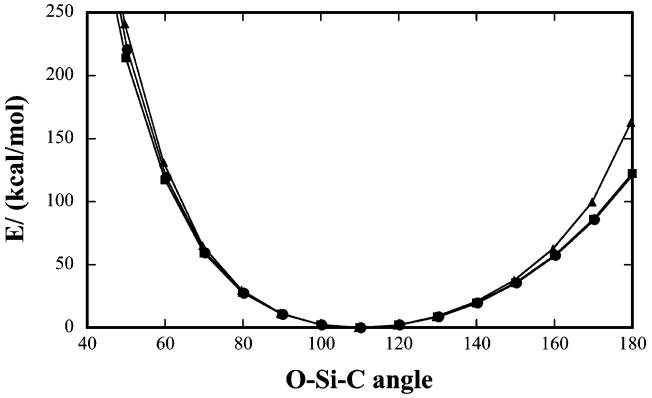

Figure 4. O−Si−C bending potentials from DFT for ethyl-POSS (filled circles), propyl-POSS (filled squares), and cyclohexyl-POSS (filled triangles) monomers.

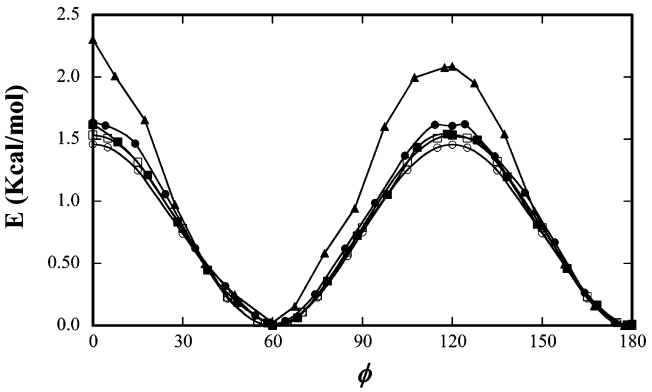

Figure 5. O−Si−C−C dihedral potentials from DFT for ethyl-POSS (filled circles), propyl-POSS (filled squares), and cyclohexyl-POSS (filled triangles) monomers. Open circles and open squares are Gaussian 98 MP2 results for ethyl- and propyl-POSS, respectively.

interactions that result from the interactions of POSS with the larger cyclohexyl group. At +50°, the potential energies of cyclohexyl-POSS, ethyl-POSS, and propyl-POSS are 33, 31, and 31 kcal/mol, respectively; at −50°, the potential energies are 79, 76, and 84 kcal/mol, respectively. Within ±20° of deviation, the differences between the three potential curves are minimal, with the energy penalty less than 12 kcal/mol. A single analytical potential can be used for all three angles within ±20° of deviation.

iv. O−Si−C−C Dihedral Potential. The calculated O−Si−C−C dihedral potentials for ethyl- (Figure 1b), propyl- (Figure 1c), and cyclohexyl-POSS (Figure 1e) monomers are reported in Figure 5. In all cases, our results show that two equilibrium angles are obtained at 60° and 180°, both corresponding to the gauche configuration in classical Newman projections whereby the terminal carbon atom prefers to align itself as far away from the POSS cage as possible (Figure 6). For the linear-hydrocarbon-substituted POSS monomers, the energy barrier to convert from one equilibrium conformation to the next is approximately 1.5 kcal/mol (equivalently $2.5k_BT$ at room temperature). This is consistent with classic organic chemistry, which shows the energy of the anti configuration of butane to be 3 kcal/mol higher than the lowest-energy gauche configuration. The influence of the constrained cyclohexane ring is quite small, increasing the barrier to 2.0 kcal/mol.

v. Si−C−C−C Dihedral Potential. In Figure 7, we report our results for the Si−C−C−C dihedral potential for propyl- (Figure 1c) and butyl-POSS (Figure 1d) and the C−C−C−C dihedral potentials for butyl-POSS and normal-butane. The dihedral potentials obtained for n-butyl-POSS and n-butane are, for all practical purposes, indistinguishable, suggesting that the presence of the POSS monomer does not alter the geometric properties of the hydrocarbon chain to which it is covalently bound. The Si −C−C−C dihedral potential obtained for propyl-POSS and butyl-POSS are indistinguishable, and both possess features similar to the C−C−C−C− dihedral obtained for the butyl-POSS and normal-butane. The most stable structure is that which occurs at a dihedral angle of 180°, and is the well-known anti conformer. The eclipsed conformer, in which the Si (POSS) and the remaining R group of the second carbon in the Newman projection sit at 60°, is also a low-energy structure but is about 1 kcal/mol less stable due to van der Waals repulsion. This is consistent with the energy difference between the anti and gauche configurations for butane alone. The structure at 120° is a maximum on the potential energy curve because the Si (POSS) and R groups now sit in the eclipsed configuration. This structure is 2.6−3.2 kcal/mol higher than that for the lowest-energy anti conformer. This is also similar to the results for simple butane. The structure at 0° is the highest in energy because it combines both the torsional strain for adopting an eclipsed structure and the van der Waals repulsive interactions between the two hydrogen atoms on the carbon atom directed toward the cage and the two oxygen atoms on the cage.

The Si−C−C−C and H−C−C−C dihedral potentials for the cyclohexyl-POSS (Figure 1e) and cyclohexane systems, shown in Figure 8, are characteristically different than those for the linear alkyl-substituted POSS. There is only one minimum

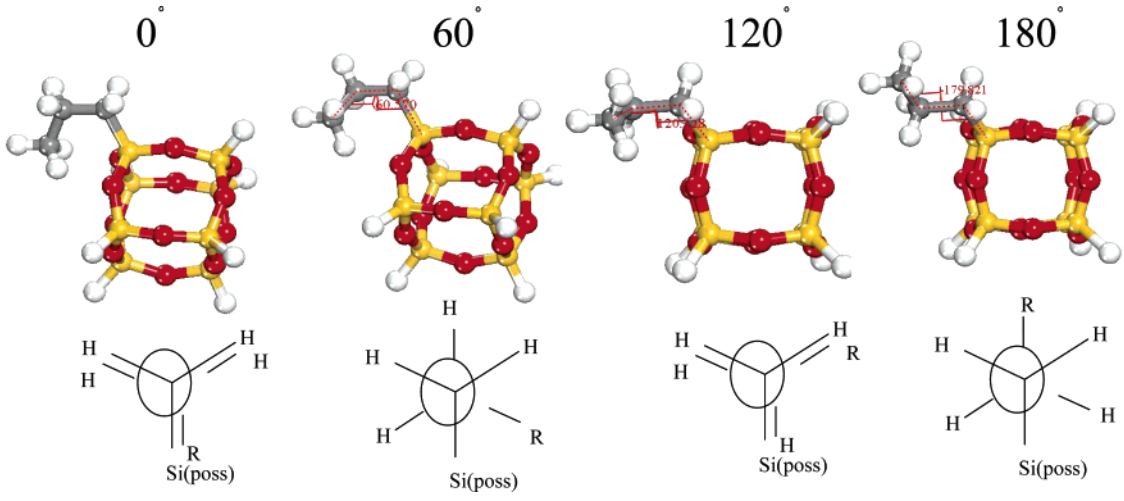

Figure 6. Newman projection plots of propyl-POSS monomer.

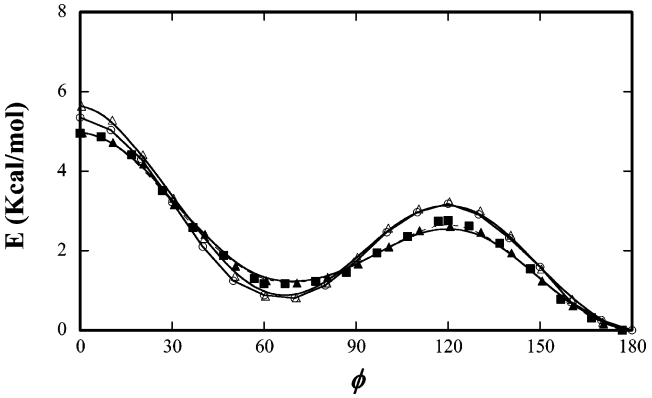

Figure 7. Dihedral potential energies from DFT for Si−C−C−C of propyl-POSS (filled squares), Si−C−C−C (filled triangles), and C−C−C−C (open triangles) of butyl-POSS. Open circles represent results obtained for the dihedral angle C−C−C−C in normal butane.

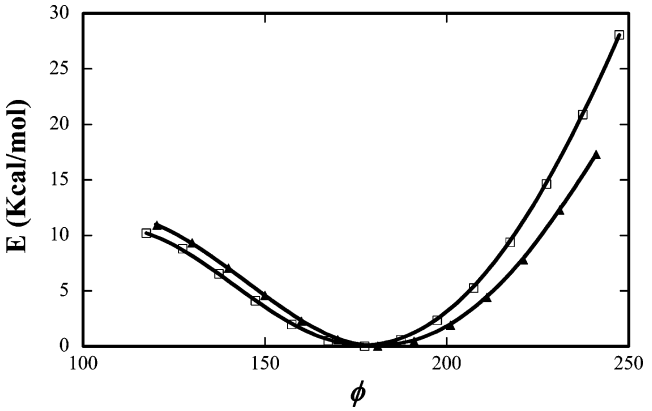

Figure 8. Comparison of H−C−C−C dihedral potential of cyclohexane (open squares) and the Si−C−C−C dihedral potential of cyclohexyl-POSS (filled triangles) from DFT.

energy at 180° for the anti conformation. All other structures are much higher in energy and unstable. This is due to the fact that changes in the Si−C−C−C dihedral angle would lead to significant changes in the actual Si−C−C bond angle, which will create strain on the ring structure and cause the POSS cage to move quite close to the cyclohexyl group, leading to substantial repulsion. A similar energy penalty is also seen for cyclohexane, where changing the H−C−C−C angle results in significant strain in the ring. A comparison of the potential curves shows that the H−C−C−C potential is slightly shallower than the Si−C−C−C potential for negative dihedral rotation; on the contrary, the Si−C−C−C potential is shallower than the H−C−C−C potential for positive dihedral rotation. This is because for negative dihedral rotation, the cyclohexyl group moves closer to the POSS cage, adding more energy penalty to the Si−C−C−C potential compared to the steric effect from only a H atom for the H−C−C−C potential. For positive dihedral rotation, the strain on the ring increases as the cyclohexyl group is moved away from the POSS cage. Cyclohexane has a larger energy penalty compared to cyclohexyl-POSS because the steric effect for cyclohexane between two H atoms sharing the same C atom is larger than the steric effect for cyclohexyl-POSS between the Si atom and the nearest H atom on the ring.

The stretching, bending, and dihedral potentials discussed in the previous paragraphs indicate that, as a first approximation, the presence of one hydrocarbon chain covalently bound to a POSS monomer does not influence significantly the geometric properties of the POSS monomer. The presence of the POSS monomer, however, can influence the properties of the hydrocarbon chain, though these differences tend to occur at much more extreme deviations from the equilibrium structure. The changes close to the optimal angles and torsion angles are not as large. The results suggest that to a first-order approximation standard alkane force fields may used to describe alkyl tethers and substituents on the POSS cage. The potentials can be improved, however, by noting the repulsive interactions that exist at negative deviations from their optimal values due to increased steric interactions.

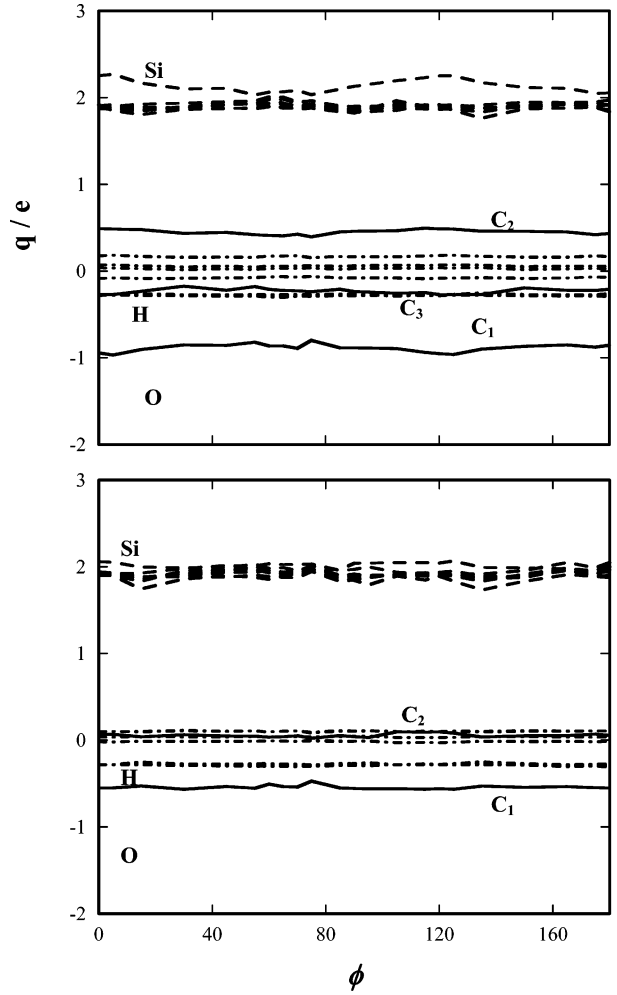

Figure 9. Partial charges localized on each atom as a function of the dihedral angle O−Si−C−C ethyl- (top) and propyl-POSS (bottom). Gray lines represent charges on silicon (broken line), oxygen (dotted line), and hydrogen (line−dot line) atoms in the POSS monomer. Black lines represent charges on carbon (continuous line) and hydrogen (dotted lines) atoms in the hydrocarbon substituents. C_1 is the carbon atom covalently bound to the Si atom in the POSS cage; C_2 is covalently bound to C_1, and so forth.

Partial Charges. Although much of our initial work on POSS monomers was performed using published force fields such as COMPASS[54] and UFF,[55] in order to develop a specific force field for POSS for use in atomistic simulations it is important to determine the partial charges localized on each atom. It is also of interest to understand if these partial charges depend on the morphology of a POSS monomer. In other words, we want to understand if the charges fluctuate when the POSS monomer undergoes certain structural motions. To investigate these points, we determined the partial charges on each of the atoms in ethyl-POSS (Figure 1b) and propyl-POSS (Figure 1c) as a function of the O−Si−C−C dihedral angle. We present the results in Figure 9. For both monomers, our results indicate that the partial charges do not significantly depend on the O−Si−C−C dihedral

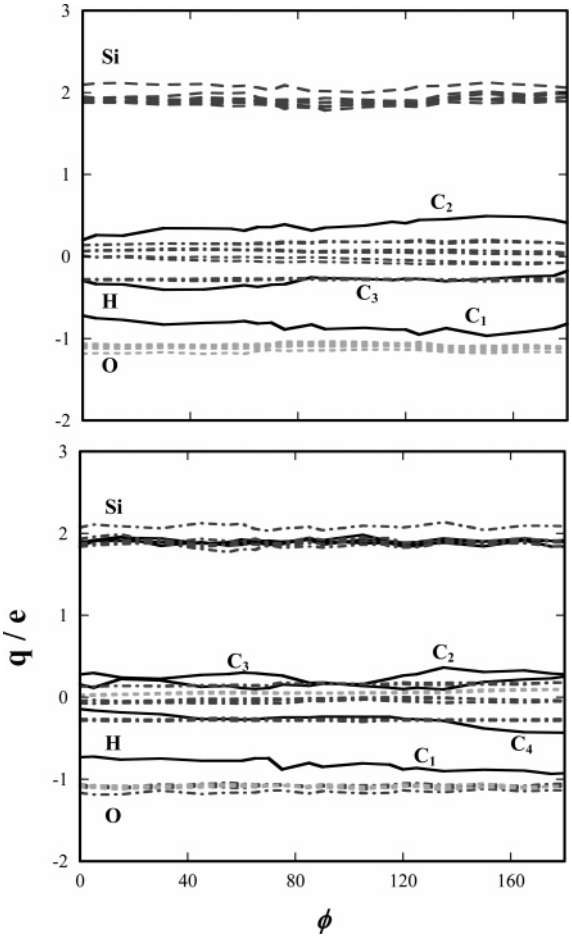

Figure 10. Partial charges localized on each atom as a function of the dihedral angle Si−C−C−C for propyl- (top) and butyl-POSS (bottom). Gray lines represent charges on silicon (broken line), oxygen (dotted line), and hydrogen (line−dot line) atoms in the POSS monomer. Black lines represent charges on carbon (continuous line) and hydrogen (dotted lines) atoms in the hydrocarbon substituents. C_1 is the carbon atom covalently bound to the Si atom in the POSS cage; C_2 is covalently bound to C_1, and so forth.

angle and that the charges located on hydrogen, silicon, and oxygen atoms in the POSS cages are essentially independent of the position considered. However, the partial charges localized on the hydrocarbon substituents depend on the position of the atom considered. In the case of the ethyl-POSS monomer, it is interesting that the carbon atom covalently bound to the silicon atom (C_1) of the POSS cage takes on a negative charge approximately equal to $-0.5e$ whereas the second carbon (C_2) is positively charged. In the propyl-POSS monomer C_1 and C_3 take on negative charges, whereas C_2 is positively charged. The charges, however, are not significantly large on any of these atoms.

We performed similar calculations for the atomic partial charges as a function of the Si−C−C−C dihedral angle for propyl- and butyl-POSS (Figure 1d) monomers. The results are shown in Figure 10. Again, the partial charges localized within the POSS monomer do not change when the dihedral angle is changed or when a different hydrocarbon chain is covalently bound to a silicon atom. The partial charges on the carbon atoms of the substituent hydrocarbon chain are perturbed by the presence of the POSS monomer. In particular, the carbon atom covalently bound to the silicon atom in the silsesquioxane monomer (C_1) always bears a negative partial charge. In Table 3, we report partial charges assigned to each atom for the POSS monomers considered in this work. The results shown in Table 3 indicate that the hydrogen atoms in each silsesquioxane take on negative partial charges. This is simply to balance the formal positive charge on the Si atoms.

Summary and Conclusions

Ab initio quantum chemical calculations have been carried out to determine the structural properties as well as the intramolecular potentials for alkyl-substituted polyhedral oligomeric silsesquioxane macromolecules. The aim of this work was to understand if the geometric features of polyhedral oligomeric silsesquioxane $(SiO_{1.5})_8H_8$ molecules are modified by substituting the terminal hydrogen atoms on the POSS cage with short hydrocarbon chains. The results show only minor changes in the minimum-energy configurations for monosubstituted POSS monomers compared to bare POSS molecules. The results indicate that the length of the linear hydrocarbon chain does not affect the structural or electronic properties of the POSS cage to which it is covalently bound.

We have also investigated how the geometric features of the hydrocarbon substituents (tethers) are modified when they are covalently attached to a single POSS molecule as compared to the free hydrocarbon. The results show that although the silsesquioxanes do not appreciably influence the geometric properties of the hydrocarbon chains near the optimized equilibrium structure, appreciable deviations are found for structures that are displaced further from their optimal structure. In particular, the more sterically hindered substituents such as cyclohexane begin to interact with the POSS at smaller bond angles and specific torsion angles. This occurs at (1) smaller Si−C−C bond angles and (2) specific O−Si−C−C and Si−C−C−C torsion angles where the cyclohexyl groups are forced to interact directly with the POSS cage. The electronic properties of the linear hydrocarbon chain substituents do not appear to be affected by the presence of the POSS cage. In particular, the partial charge assigned to the carbon atom covalently bound to the silicon atom in the POSS monomer is always negative.

The results presented here show that the standard hydrocarbon and silica force fields can be used as a first approximation to describe the alkyl-POSS systems. These potentials, however, can be improved upon, by recognizing and accounting for the steric influences between the bulkier ring substituents and the silica cage at shorter bond angles and specific torsion angles.

TABLE 3: Atomic Partial Charges Calculated for the Plain POSS and Linear Alkyl-Tethered POSS Monomers Considered in This Work[a]

	Si	O	H_{POSS}	C_1	H_1	C_2	H_2	C_3	H_3	C_4	H_4
POSS	1.93	−1.10	−0.28								
ethyl-POSS	1.95	−1.11	−0.29	−0.53	−0.01	0.06	0.08				
propyl-POSS	1.94	−1.10	−0.28	−0.86	0.16	0.42	−0.07	−0.22	0.04		
butyl-POSS	1.91	−1.08	−0.28	−0.90	0.17	0.26	−0.05	0.25	−0.04	−0.40	0.09

[a] Partial charges are expressed in atomic units. C_1 is the carbon atom covalently bound to the Si atom in the POSS cage; C_2 is covalently bound to C_1, and so forth. H1 indicates the hydrogen atoms covalently bound to C_1; H_2 indicates hydrogen atoms covalently bound to C_2, and so forth. H_{POSS} indicates the hydrogen atoms covalently bound to the silicon atoms in the silsesquioxane monomer.

These potentials can ultimately be used in classical molecular dynamic simulations and/or Monte Carlo studies in order to determine the thermodynamic properties of these organic/inorganic hybrid silsesquioxane systems.

Acknowledgment. We acknowledge financial support from the U.S. National Science Foundation under grant no. DMR-0103399. Calculations were performed on the VAMPIRE cluster at Vanderbilt University and at the NERSC facilities, Berkeley, CA.

References and Notes

(1) Phillips, S. H.; Haddad, T. S.; Tomczak, S. J. *Current Opinion in Solid State & Materials Science* **2004**, *8* (1), 21−29.
(2) Lichtenhan, J. D.; Vu, N. Q.; Carter, J. A.; Gilman, J. W.; Feher, F. J. *Macromolecules* **1993**, *26*, 2141.
(3) Fu, B. X.; Hsiao, B. S.; Pagola, S.; Stephens, P.; White, H.; Rafailovich, M.; Sokolov, J.; Mather, P. T.; Jeon, H. G.; Phillips, S.; Lichtenhan, J.; Schwab, J. *Polymer* **2001**, *42*, 599.
(4) Xu, H. Y.; Kuo, S. W.; Lee, J. S.; Chang, F. C. *Macromolecules* **2002**, *35*, 8788.
(5) Wang, J. S.; Matyjaszewski, K. *J. Am. Chem. Soc.* **1995**, *117*, 5614.
(6) Pan, G. R.; Mark, J. E.; Schaefer, D. W. *J. Polym. Sci., Part B: Polym. Phys.* **2003**, *41*, 3314.
(7) Carroll, J. B.; Frankamp, B. L.; Rotello, V. M. *Chem. Commun.* **2002**, 1892.
(8) Naka, K.; Itoh, H.; Chujo, Y. *Nano Lett.* **2002**, *2*, 1183.
(9) Carroll, J. B.; Frankamp, B. L.; Srivastava, S.; Rotello, V. M. *J. Mater. Chem.* **2004**, *14*, 690.
(10) Cassagneau, T.; Caruso, F. *J. Am. Chem. Soc.* **2002**, *124*, 8172.
(11) Bellas, V.; Tegou, E.; Raptis, I.; Gogolides, E.; Argitis, P.; Iatrou, H.; Hadjichristidis, N.; Sarantopoulou, E.; Cefalas, A. C. *J. Vac. Sci. Technol., B* **2002**, *20*, 2902.
(12) Leu, C. M.; Chang, Y. T.; Wei, K. H. *Macromolecules* **2003**, *36*, 9122.
(13) Leu, C. M.; Reddy, G. M.; Wei, K. H.; Shu, C. F. *Chem. Mater.* **2003**, *15*, 2261.
(14) Shockey, E. G.; Bolf, A. G.; Jones, P. F.; Schwab, J. J.; Chaffee, K. P.; Haddad, T. S.; Lichtenhan, J. D. *Appl. Organomet. Chem.* **1999**, *13*, 311.
(15) Lichtenhan, J. D. *Comments Inorg. Chem.* **1995**, *17*, 115.
(16) Choi, J.; Yee, A. F.; Laine, R. M. *Macromolecules* **2003**, *36*, 5666.
(17) Bharadwaj, R. K.; Berry, R. J.; Farmer, B. L. *Polymer* **2000**, *41*, 7209.
(18) Ionescu, T.; Qi, F.; McCabe, C.; Striolo, A.; Kieffer, J.; Cummings, P. T. *J. Phys. Chem. B* **2006**, *110*, 2502.
(19) Peng, Y.; McCabe, C. *Mol. Phys.* **2007**, *105*, 261−272.
(20) Striolo, A.; McCabe, C.; Cummings, P. T. *Macromolecules* **2005**, *38*, 8950.
(21) Striolo, A.; McCabe, C.; Cummings, P. T. *J. Phys. Chem. B* **2005**, *109*, 14300.
(22) Striolo, A.; McCabe, C.; Cummings, P. T. *J. Chem. Phys.* **2006**, *125*, 104504.
(23) (a) Striolo, A.; McCabe, C.; Cummings, P. T.; Chan, E. R.; Glotzer, S. C. *J. Phys. Chem. B* **2007**, submitted for publication. (b) Chan, E. R.; Striolo, A.; McCabe, C.; Glotzer, S. C.; Cummings, P. T. *J. Chem. Phys.* **2007**, submitted for publication.
(24) Hill, J. R.; Sauer, J. *J. Phys. Chem.* **1994**, *98*, 1238.
(25) Kudo, T.; Gordon, M. S. *J. Am. Chem. Soc.* **1998**, *120*, 11432.
(26) Xiang, K. H.; Pandey, R.; Pernisz, U. C.; Freeman, C. *J. Phys. Chem. B* **1998**, *102*, 8704.
(27) Earley, C. W. *J. Phys. Chem.* **1994**, *98*, 8693.
(28) Wichmann, D.; Jug, K. *J. Phys. Chem. B* **1999**, *103*, 10087.
(29) Pasquarello, A.; Hybertsen, M. S.; Car, R. *Phys. Rev. B* **1996**, *54*, R2339.
(30) Sasamori, R.; Okaue, Y.; Isobe, T.; Matsuda, Y. *Science* **1994**, *265*, 1691.
(31) Mattori, M.; Mogi, K.; Sakai, Y.; Isobe, T. *J. Phys. Chem. A* **2000**, *104*, 10868.
(32) Tejerina, B.; Gordon, M. S. *J. Phys. Chem. B* **2002**, *106*, 11764.
(33) Duchateau, R.; Abbenhuis, H. C. L.; van Santen, R. A.; Meetsma, A.; Thiele, S. K. H.; van Tol, M. F. H. *Organometallics* **1998**, *17*, 5663.
(34) Murugavel, R.; Voigt, A.; Walawalkar, M. G.; Roesky, H. W. *Chem. Rev.* **1996**, *96*, 2205.
(35) Kudo, T.; Gordon, M. S. *J. Phys. Chem. A* **2001**, *105*, 11276.
(36) Franco, R.; Kandalam, A. K.; Pandey, R.; Pernisz, U. C. *J. Phys. Chem. B* **2002**, *106*, 1709.
(37) Knischka, R.; Dietsche, F.; Hanselmann, R.; Frey, H.; Mulhaupt, R.; Lutz, P. J. *Langmuir* **1999**, *15*, 4752.
(38) Frisch, M. J.; Trucks, G. W.; Schlegel, H. B.; Scuseria, G. E.; Robb, M. A.; Cheeseman, J. R.; Zakrzewski, V. G.; Montgomery, J. A., Jr.; Stratmann, R. E.; Burant, J. C.; Dapprich, S.; Millam, J. M.; Daniels, A. D.; Kudin, K. N.; Strain, M. C.; Farkas, O.; Tomasi, J.; Barone, V.; Cossi, M.; Cammi, R.; Mennucci, B.; Pomelli, C.; Adamo, C.; Clifford, S.; Ochterski, J.; Petersson, G. A.; Ayala, P. Y.; Cui, Q.; Morokuma, K.; Malick, D. K.; Rabuck, A. D.; Raghavachari, K.; Foresman, J. B.; Cioslowski, J.; Ortiz, J. V.; Stefanov, B. B.; Liu, G.; Liashenko, A.; Piskorz, P.; Komaromi, I.; Gomperts, R.; Martin, R. L.; Fox, D. J.; Keith, T.; Al-Laham, M. A.; Peng, C. Y.; Nanayakkara, A.; Gonzalez, C.; Challacombe, M.; Gill, P. M. W.; Johnson, B. G.; Chen, W.; Wong, M. W.; Andres, J. L.; Head-Gordon, M.; Replogle, E. S.; Pople, J. A. *Gaussian 98*, revision A.9; Gaussian, Inc.: Pittsburgh, PA, 1998.
(39) Delley, B. *J. Chem. Phys.* **2000**, *113*, 7756.
(40) Hammer, B.; Hansen, L. B.; Norskov, J. K. *Phys. Rev. B* **1999**, *59*, 7413.
(41) Mulliken, R. S. *J. Chem. Phys.* **1955**, *23*, 1833.
(42) Singh, U. C.; Kollman, P. A. *J. Comput. Chem.* **1984**, *5*, 129.
(43) Weiner, S. J.; Kollman, P. A.; Nguyen, D. T.; Case, D. A. *J. Comput. Chem.* **1986**, *7*, 230.
(44) Weiner, S. J.; Kollman, P. A.; Case, D. A.; Singh, U. C.; Ghio, C.; Alagona, G.; Profeta, S.; Weiner, P. *J. Am. Chem. Soc.* **1984**, *106*, 765.
(45) Cox, S. R.; Williams, D. E. *J. Comput. Chem.* **1981**, *2*, 304.
(46) Momany, F. A. *J. Phys. Chem.* **1978**, *82*, 592.
(47) Reynolds, C. A.; Essex, J. W.; Richards, W. G. *Chem. Phys. Lett.* **1992**, *199*, 257.
(48) Reynolds, C. A.; Essex, J. W.; Richards, W. G. *J. Am. Chem. Soc.* **1992**, *114*, 9075.
(49) Bayly, C. I.; Cieplak, P.; Cornell, W. D.; Kollman, P. A. *J. Phys. Chem.* **1993**, *97*, 10269.
(50) Besler, B. H.; K. M. Merz, J.; Kollman, P. A. *J. Comput. Chem.* **1990**, *11*, 431.
(51) Auf der Heyde, T. P. E.; Burgi, H. B.; Burgy, H.; Tornroos, K. W. *Chimia* **1991**, *45*, 38.
(52) Earley, C. W. *Inorg. Chem.* **1992**, *31*, 1250.
(53) Tornroos, K. W. *Acta Crystallogr., Sect. C* **1994**, *50*, 1646.
(54) Sun, H. *J. Phys. Chem. B* **1998**, *102*, 7338.
(55) Rappe, A. K.; Casewit, C. J.; Colwell, K. S.; Goddard, W. A.; Skiff, W. M. *J. Am. Chem. Soc.* **1992**, *114*, 10024.
(56) Lin, T.; He, C.; Xiao, Y. *J. Phys. Chem. B* **2003**, *107*, 13788.